NINETEENTH EUROPEAN ROTORCRAFT FORUM

Paper n°: M1

IMPROVED EPICYCLIC GEAR ANALYSIS ALGORITHMS

by

A. Bellazzi, B. Maino, S. Mancin

AGUSTA, ITALY

September 14-16, 1993
CERNOBBIO (Como)
ITALY

ASSOCIAZIONE INDUSTRIE AEROSPAZIALI
ASSOCIAZIONE ITALIANA DI AERONAUTICA ED ASTRONAUTICA

IMPROVED EPICYCLIC GEAR ANALYSIS ALGORITHMS

A. Bellazzi, B. Maino, S. Mancin

AGUSTA

The analysis of the sun and planet epicyclical gears is one of the most demanding aspects of the transmission vibration monitoring; also the EH101 epicyclical stage, composed by a fixed external ring and six planets surrounding a central sun gear, presents some peculiar analysis difficulties.

State-of-the-art algorithms, which are successfully used to provide early failure detection in other gears, show unacceptable performances when applied to this stage of the transmission.

Dedicated analysis techniques for the epicyclical gears have been developed: the key aspect is the time-averaging algorithm; this is a commonly used procedure to remove from the analyzed signal any contribution that is not synchronous with the rotation frequency of the gear being analyzed.

The standard application of the time-average procedure, without taking into account the complex kinematic of the epicycle assembly, does not guarantee satisfactory results. The modified procedure, instead of averaging any acquired buffer regardless of the actual position of the gears, allows the selection of the buffers according to the instantaneous position of the epicycle gears with reference to the accelerometer.

It is therefore possible to focus the health analysis on the single planet or on a particular sector of the sun gear when their meshing occurs close to the accelerometer. This approach guarantees the improvement of both the averaging performances and the visibility of potential defects.

Several types of signals have been used to assess the algorithm performances, ranging from flight recordings on different EH101 prototypes, to ground transmission tests with different levels of artificially introduced faults (with the removal of 20, 50, 70% of the casehardening surface of both sun and planet gears).

The confrontation with the conventional analysis results shows that significative improvement in the early failure detection can be achieved with the application of the developed techniques.

1. INTRODUCTION

Among the transmission Health Monitoring techniques, Vibration Monitoring is getting more and more important because it is considered able to detect failures otherwise not detectable. This feature makes Vibration Monitoring Systems essential both to improve the flight safety and to aim at on-condition maintenance.

Considerable effort is continuously dedicated to the research of more efficient analysis techniques [2-7], resulting in the development of new and more effective techniques, but the health monitoring of some particular items is still problematical.

The analysis of the epicyclical gears (i.e., sun and planets) is one of the most demanding aspects of the transmission health status monitoring.

Even the state-of-the-art algorithms, which can be successfully used to provide early failure detection in other gears, show unacceptable performances when applied to this stage of the transmission. This poor effectiveness is mainly related to the characteristics of the analysed signals: the vibrations get by the accelerometer results from all of the twelve ring-planet and sun-planet contacts that have the same mesh frequency. The different phases of each signal cause cancellation or amplifications in relation with the different frequencies [1]. Furthermore, any pulse related to the meshing of a defective tooth is averaged with the "normal" vibrations of all of the other contacts.

Especially when the defective meshing occurs far from the accelerometer location, it can be expected that its contribution to the sensed vibration is almost inappreciable.

As already mentioned, in consequence of these peculiar characteristics, the conventional analysis techniques do not give satisfactory performance in terms of early failure detection.

The algorithms developed by Agusta for sun and planet analysis consist in both an improved time-averaging procedure and a tailoring of the signal enhancement process with spectral reduction. Their application results in a considerable improvement of the early failure detection for the epicyclical stage gears.

2. EH101 TRANSMISSION VIBRATION MONITORING SYSTEM

EH101 is being provided with a vibration monitoring capability and for this reason the gearbox system is fitted with 15 accelerometers and 2 azimuth sensors.

The adopted analysis procedure entails the sampling of the raw accelerometer signal at the appropriate frequency, with each buffer covering

exactly one gear revolution with 2^N samples (N chosen in relation with the gear number of teeth). The buffers are time-averaged together, aiming at removing both noise and the other gears' meshing vibrations. This procedure reduces all the signal components that are not exactly synchronous with the analyzed gear revolution. The averaged buffer is then analyzed with different algorithms dedicated to the detection of anomalous peaks, phase deviations, 1xRev. vibrations and modifications in the spectral amplitude distribution.

On the basis of the current experience, the vibration monitoring is expected to highlight at least the following failure modes:

Gears:
- •tooth breakage (complete of one tooth, partial of some teeth)
- •two or more consecutive teeth breakage
- •body breakage
- •destructive pitting,
- •heavy scoring, accelerated wear
- •spalling (with the loss of a noticeable part of the load carrying surface)

Shafts:
- •unbalance
- •misalignment
- •shaft, flange and/or web breakage

Bearings:
- •seizure
- •severe scoring, spalling, flaking
- •breakage of ball/rollers, cage or racers
- •breakage involving bearing seat

The conservative approach to survey only some of the identified failure modes with the vibration monitoring techniques does not prevent the complete coverage of the most critical failures. It must be reminded that the whole transmission health monitoring includes several systems (e.g., QDM, oil temperature monitoring, bearing temperature monitoring, torque and speed monitoring) that are sensitive to different failure effects.

3. DATA SOURCES

Several types of signals have been used in the algorithm development phase, ranging from test rig recordings with different levels of artificially introduced damages on both sun and planet gears, to flight recordings on different EH101 prototypes.

The available data can be splitted up into four groups, according to the level of tooth damage (implying different levels of expected analysis results):

BASELINE DATA: data of this group come from transmissions with gears in good conditions, as reported by periodic inspections; it is therefore expected that the analysis results do not exceed a reasonably low threshold (the precise value will be defined after the achievement of a sufficient confidence on the algorithm performances).

LOW SEEDED FAULTS: data of this group come from HUM dedicated recordings of transmissions tested on the Agusta rig, where the 15÷20% of the casehardening surface of one tooth is removed. It is not expected at this stage of the research to be the able to highlight such little defects in the epicyclical stage (this level of artificial damage, roughly corresponding to either a spall or a little crack, can be detected by the algorithms currently employed when applied to simple two gears meshings).

MEDIUM SEEDED FAULTS: for these recordings the 50% of the tooth casehardening surface has been removed. It is expected that the analysis results will almost always identify the presence of the defect (this means that the analysis output values shall be well above the normal baseline values).

LARGE SEEDED FAULTS: for these recordings the 70% of the tooth casehardening surface has been removed (even if not tested, it is believed that such a large damage should lead to the complete tooth breakage in a short period). It is expected that the analysis procedure will always identify the presence of this defect (the analysis output values must be well above the normal baseline values).

SUN SIGNALS		
Ref. Name	**A**	**Description**
PP7SLA08	8	EH101 PP7 - flight 114 - Level flight 100 kts
PP7SLA09	9	EH101 PP7 - flight 114 - Level flight 100 kts
PP7SLA10	10	EH101 PP7 - flight 114 - Level flight 100 kts
PP7SHA08	8	EH101 PP7 - flight 114 - Hovering
PP7SHA09	9	EH101 PP7 - flight 114 - Hovering
PP7SHA10	10	EH101 PP7 - flight 114 - Hovering
PP2SLA08	8	EH101 PP2 - flight 448 - Level flight 100 kts
PP2SLA09	9	EH101 PP2 - flight 448 - Level flight 100kts
PP2SLA10	10	EH101 PP2 - flight 448 - Level flight 100kts
PP2SHA08	8	EH101 PP2 - flight 448 - Hovering OGE
PP2SHA09	9	EH101 PP2 - flight 448 - Hovering OGE
PP2SHA10	10	EH101 PP2 - flight 448 - Hovering OGE
PP6SHA08	8	EH101 PP6 - flight 159 - Hovering OGE
BAS20S08	8	Rig baseline rec.: 3640HP (s.f. on planet 20%)
BAS20S09	9	Rig baseline rec.: 3640HP (s.f. on planet 20%)
BAS20S10	10	Rig baseline rec.: 3640HP (s.f. on planet 20%)
BAS20S82	8	Rig baseline rec.: 4400HP (s.f. on planet 20%)
BAS20S83	8	Rig baseline rec.: 4885HP (s.f. on planet 20%)
BAS70S08	8	Rig baseline rec.: 3640HP (s.f. on planet 70%)
BAS70S09	9	Rig baseline rec.: 3640HP (s.f. on planet 70%)
BAS70S10	10	Rig baseline rec.: 3640HP (s.f. on planet 70%)
BAS70S82	8	Rig baseline rec.: 4400HP (s.f. on planet 70%)
BAS70S83	8	Rig baseline rec.: 4885HP (s.f. on planet 70%)
SUN20A08	8	Rig rec.: seeded fault on sun 20%; 3640HP
SUN20A09	9	Rig rec.: seeded fault on sun 20%; 3640HP
SUN20A10	10	Rig rec.: seeded fault on sun 20%; 3640HP
SUN20A82	8	Rig rec.: seeded fault on sun 20%; 4400HP
SUN20A83	8	Rig rec.: seeded fault on sun 20%; 4885HP
SUN50A08	8	Rig rec.: seeded fault on sun 50%; 3640HP
SUN50A09	9	Rig rec.: seeded fault on sun 50%; 3640HP
SUN50A10	10	Rig rec.: seeded fault on sun 50%; 3640HP
SUN50A82	8	Rig rec.: seeded fault on sun 50%; 4400HP
SUN50A83	8	Rig rec.: seeded fault on sun 50%; 4885HP
SUN70A08	8	Rig rec.: seeded fault on sun 70%; 3640HP
SUN70A09	9	Rig rec.: seeded fault on sun 70%; 3640HP
SUN70A10	10	Rig rec.: seeded fault on sun 70%; 3640HP
SUN70A82	8	Rig rec.: seeded fault on sun 70%; 4400HP
SUN70A83	8	Rig rec.: seeded fault on sun 70%; 4885HP

Table 1a: Summary of the analysed signals - SUN

Table 1 lists the complete set of signals used to test the developed procedures, together with the reference names that will be used throughout the document.

Three accelerometers (No 8,9 and 10) are fitted on the main gear box to monitor the epicyclical stage; the new algorithm requires only one signal to monitor planet and sun health. Aiming at selecting which accelerometer can give the results in terms of resolution between baseline and seeded fault values, a subset of vibration signals from accelerometers 9 and 10 have been analyzed together with accelerometer 8 signals.

As a result of the first assessment, accelerometer 8 seems to give slightly better results when compared to the other two, therefore it has been chosen as default for the analyses (with number 10 as back-up device).

It can be remarked that the seeded fault signals for the planet are the baseline values for the sun gear and vice versa. This procedure should not surprise because the time-average procedure removes every signal that is not synchronous with the revolution period of the gear being tested; hence, the pulses of other gears' damaged teeth will not affect the averaged signal of the gear being monitored.

PLANET SIGNALS		
Ref. Name	A	Description
PP7PLA08	8	EH101 PP7 - flight 114 - Level flight 100 kts
PP7PLA09	9	EH101 PP7 - flight 114 - Level flight 100 kts
PP7PLA10	10	EH101 PP7 - flight 114 - Level flight 100 kts
PP7PLA1B	10	As above (PP7PLA10); 2nd acquisition
PP7PHA08	8	EH101 PP7 - flight 114 - Hovering
PP7PHA09	9	EH101 PP7 - flight 114 - Hovering
PP7PHA10	10	EH101 PP7 - flight 114 - Hovering
PP2PLA08	8	EH101 PP2 - flight 448 - Level flight 100 kts
PP2PLA09	9	EH101 PP2 - flight 448 - Level flight 100kts
PP2PLA10	10	EH101 PP2 - flight 448 - Level flight 100kts
BAS20P08	8	Rig baseline rec.: 3640HP (s.f. on sun 20%)
BAS20P09	9	Rig baseline rec.: 3640HP (s.f. on sun 20%)
BAS20P10	10	Rig baseline rec.: 3640HP (s.f. on sun 20%)
BAS20P82	8	Rig baseline rec.: 4400HP (s.f. on sun 20%)
BAS20P83	8	Rig baseline rec.: 4885HP (s.f. on sun 20%)
BAS70P08	8	Rig baseline rec.: 3640HP (s.f. on sun 70%)
BAS70P09	9	Rig baseline rec.: 3640HP (s.f. on sun 70%)
BAS70P10	10	Rig baseline rec.: 3640HP (s.f. on sun 70%)
BAS70P82	8	Rig baseline rec.: 4400HP (s.f. on sun 70%)
BAS70P83	8	Rig baseline rec.: 4885HP (s.f. on sun 70%)
PLA20A08	8	Rig rec.: seeded fault on planet 20%; 3640HP
PLA20A09	9	Rig rec.: seeded fault on planet 20%; 3640HP
PLA20A10	10	Rig rec.: seeded fault on planet 20%; 3640HP
PLA20A82	8	Rig rec.: seeded fault on planet 20%; 4400HP
PLA20A83	8	Rig rec.: seeded fault on planet 20%; 4885HP
PLA50A08	8	Rig rec.: seeded fault on planet 50%; 3640HP
PLA50A09	9	Rig rec.: seeded fault on planet 50%; 3640HP
PLA50A10	10	Rig rec.: seeded fault on planet 50%; 3640HP
PLA50A82	8	Rig rec.: seeded fault on planet 50%; 4400HP
PLA50A83	8	Rig rec.: seeded fault on planet 50%; 4885HP
PLA70A08	8	Rig rec.: seeded fault on planet 70%; 3640HP
PLA70A09	9	Rig rec.: seeded fault on planet 70%; 3640HP
PLA70A10	10	Rig rec.: seeded fault on planet 70%; 3640HP
PLA70A82	8	Rig rec.: seeded fault on planet 70%; 4400HP
PLA70A83	8	Rig rec.: seeded fault on planet 70%; 4885HP

Table 1b: Summary of the analized signals - PLANET

4. CONVENTIONAL ANALYSIS RESULTS

In order to have a reference in the assessment of the improved analysis procedures, this paragraph presents the results of the conventional algorithms applied to a significant subset of data.

The analysis technique applied to the epicyclical gears is the so-called "spectral reduction". In the current implementation, the averaged buffer is manipulated by lowering selected spectral components. The modified spectrum, after low-pass filtering, is again transformed into the time domain. The final processing is the computation of the momentum of order six of the enhanced signal, M6A.

This parameter is particularly sensitive to irregularities and spikeness in the analyzed buffers, as those produced by localized defects on gear surface.

For sun and planet gears the buffer length corresponds, rather than to the shaft rotation period, to the interval between two successive meshing of the same tooth with the ring for the planet or with two successive planets for the sun.

In the current implementation of the analysis algorithm, 256 and 1024 samples' buffers are used for sun and planet respectively. Different parameters are also used in the spectral reduction.

The main analysis results applied to a significative subset of data (a baseline recording plus three fault levels) are summarized in table 2, where:

NA: number of averages to achieve convergence (max 130);
CV: convergence value (limit=0.08);
M6A: momentum of order 6 of the enhanced signal;

SUN				PLANET			
Signal	NA	CV	M6A	Signal	NA	CV	M6A
BAS20P08	100	0.075	7.7	BAS20S08	55	0.077	12.4
SUN20A08	125	0.079	20.6	PLA20A08	55	0.076	12.6
SUN50A08	105	0.078	13.6	PLA50A08	60	0.074	13.5
SUN70A08	130*	0.095	8.5	PLA70A08	90	0.076	12.6

* convergence not achieved

Table 2: Conventional analysis results

Evidently the conventional approach has little effectiveness when applied to epicyclical gears: the convergence of the signal cannot always be achieved. The worst aspect lies in the quality of the averaged signal. Even defects as large as the 70% seeded faults do not raise the M6A value: the conventional procedure seems not warrant any early failure detection capability.

Figure 1 shows the raw signal of the 70% sun seeded fault test as acquired by accelerometer 8. The signal is already sampled at the appropriate frequency and it is ready to be time-averaged. This means that the first buffer (samples from 1 to 256) will be summed to the second (samples from 257 to 512) and so on, up to the achievement of either the convergence or the maximum number of averages (currently 130).

The 2500 plotted samples refer to slightly more than two complete sun revolutions (1 revolution corresponding to 1140 samples). With the chosen sampling frequency signal, the meshing with the seeded fault occurs with a 256 samples' periodicity and is indicated with a triangle on the bottom part of the plot.

The figure helps to highlight the reasons of the above mentioned problems:

- the difficulties in achieving the convergence are mainly related to the low frequency oscillations that are clearly visible in the plot. These oscillations, which are related to the planet passage in front of the accelerometer, are not synchronous with either sun or planet acquisitions. The large differences in the buffers being averaged cause the described convergence difficulties.
  Hence, an appropriate selection of the averaged buffers (i.e., choosing only buffers with "similar" signals) can improve the convergence achievement.
- it is evident that the damaged tooth mesh is not always clearly visible. The reason of this characteristic lies in the complexity of the epicyclical stage of the transmission: the accelerometer senses the sum of the meshing vibrations generated by the twelve planet-ring and planet-sun contacts, with different attenuation according to the different signal transmission paths. It can be easily understood that, when the meshing of the seeded fault is far from the accelerometer location, the corresponding signal is exceeded by the other, closer, tooth meshes.
  The conventional procedure averages buffers with large pulses of the damaged tooth with buffers with negligible ones. The final result is that, especially with small defects, the averaged signal can not fully reveal the presence of signal anomalies that are detected by the signal enhancement procedures. *Misleading low M6A values are then* computed as listed in table 2. Also for this problem, an appropriate selection of the averaged buffers (i.e., choosing only the buffers characterized by the meshing of the damaged tooth close to the accelerometer) can maximize the detectability of failures.

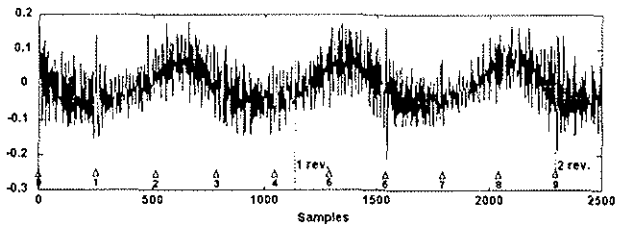

Fig.1: 70% seeded fault on sun gear; acc. 8 raw signal

5. DEDICATED TIME AVERAGE PROCEDURE

As highlighted by the preceding paragraph, the conventional time-average procedure, which uses all of the buffers for the computation of the time average, *is not adequate for epicyclical gears' analyses.* The proper selection of the buffers used in the time average procedure could greatly improve both the averaging convergence and the early failure detection capability.

Therefore, a new time average procedure has been developed and tested. The key concept of this dedicated algorithm is the selection of the averaged buffers according to their meshing position with respect to the accelerometer. Since the kinematic properties of the epicyclical assembly are known, it is possible to compute the gear position corresponding to each buffer with respect to the initial position. Hence it is possible to select a sequence of buffers characterized by the desired similarity and also corresponding to the meshing of a given planet (or portion of sun gear for the sun analysis) close to the accelerometer.

Considering the kinematic properties of the gear assembly, two successive meshings of a given sun tooth with a planet occur after a $\Theta_s=\pi/3\times(Z_R+Z_S)/Z_R$ rad sun rotation, where Z_R and Z_S are the number of teeth of the ring and sun respectively.

On the other hand, two successive meshings of a given planet tooth with the ring occur after a $\Theta_P=2\pi\times Z_P/Z_R$ rad planet carrier rotation (Z_P being the number of planet gear teeth).

Starting from the initial, reference position indicated with P_0 and S_0 in figure 2, the successive meshings of the same planet or sun tooth occur in the positions indicated with P_1 and S_1 which, for the EH101 planetary, are respectively 81 and 112 deg apart from the initial position. It should be noted that the sun meshing positions S_0, S_1, S_2, etc., take place with different and adjacent planets.

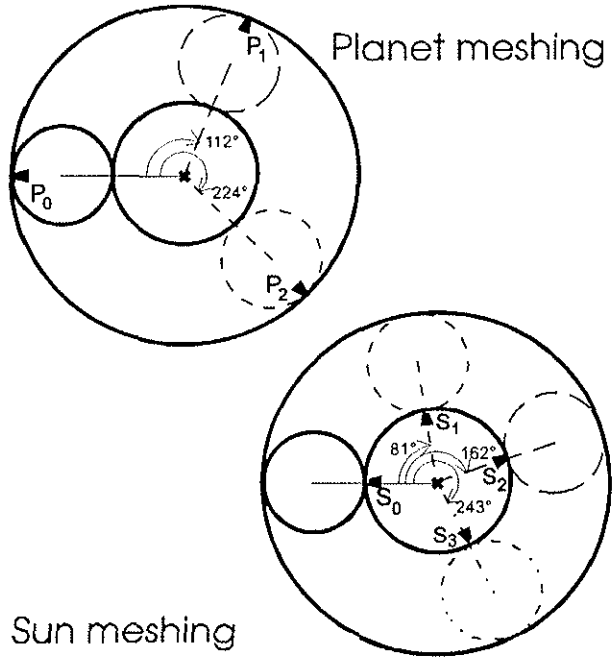

Fig.2: Successive meshing position of a given planet and sun tooth.

It is therefore possible to select the sequence of buffers characterized by similar meshing positions, satisfying the conditions:

$$-\Theta_{LS} < [(N_b-1)\times\Theta_S]\,|_{mod\ 360} < \Theta_{LS}$$

$$-\Theta_{LP} < [(N_b-1)\times\Theta_P]\,|_{mod\ 360} < \Theta_{LP}$$

for sun and planet respectively.

In the previous formulas N_b indicates the progressive buffer acquisition number. The initial angle of the first acquired buffer (N_b=1) is considered the reference position and therefore is characterized by Θ=0.

Θ_{LS} and Θ_{LP} represent the limit angles for the similarity measure, i.e. the largest acceptable angular difference between the buffers used in the average computation and the first acquired buffer. All the buffers characterized by an angular difference larger than the accepted limit are discarded and are not taken into account for the computation of the time average.

Tables 3 and 4 list the buffer sequence computed with Θ_{LS} and Θ_{LP} = 10 deg.

SUN: initial angle from -10.0 to 10.0 deg									
1	10	41	50	90	99	130	139	148	179
188	228	237	268	277	286	317	326	366	375
406	415	424	455	464	504	513	544	553	562
593	602	642	651	682	691	700	731	740	780
789	820	829	838	869	878	918	927	958	967
976	1007	1016	1056	1065	1096	1105	1114	1145	1154

Table 3: Sun analysis; buffers with initial angle from -10.0 to 10.0 deg

PLANET: initial angle from -10.0 to 10.0 deg									
1	17	46	62	78	94	123	139	155	184
200	216	232	261	277	293	322	338	354	370
399	415	431	460	476	492	508	537	553	569
598	614	630	646	675	691	707	736	752	768
784	813	829	845	874	890	906	922	951	967
983	1012	1028	1044	1060	1089	1105	1121	1150	1166

Table 4: Planet analysis; buffers with initial angle from -10.0 to 10.0 deg

As discussed below, the consequences are both the improvement of the convergence process and the capability of averaging buffers where the possible failure pulses are maximized.

In the planet analysis, this method allows to average the buffers related to each one of the 6 planets, also selecting those with angular position differing no more than an arbitrary angle with respect to the first selected buffer.

In the sun analysis, the new method is used to focus the analysis on a limited angular sector of the sun gear, i.e., only the buffers related to the selected sector and facing the accelerometer (differing less than an arbitrary angle) are used in the average. It is evident the difference with the conventional procedure, where the signals of all of the 6 planets (and all of the sun sectors) were averaged together.

On the other hand, the new method requires to perform 6 averages to analyse all of the planets and at least 4 averages for a single sun revolution.

The increment in the required analysis time is however broadly compensated by the improvement in the early failure detection capabilities.

The listed buffers refer to the first planet or sun sector. The averages relevant to the other planets or sun sectors can be computed by skipping at the beginning of the raw time history a number of samples corresponding to the angular separation among the planets or sun sectors.

Since the six planets are equally spaced by 60 degrees, 548 samples must be skipped for each planet.

For the sun, as it will be discussed later, it has been chosen to analyze 8 sectors with 90 degrees of angular increase, thus covering 2 sun revolutions. The selected angular increase correspond to a 285 samples shift for each sector.

Once shifted by the appropriate number of samples, the time averaged buffer can be computed using the same sequence of valid buffers as displayed in tables 3 and 4.

6. DATA ANALYSIS

6.1 DATA AVERAGING

One of the key factors in the early detection of failures in the epicyclical gears is the availability of a "good" signal, and this is achieved in the new time-average process by choosing buffers that have an adequate similarity.

The degree of similarity is controlled by the amplitude of the maximum angular displacement of each buffer from the initial reference position, Θ_{LS} and Θ_{LP}.

The selection of the limit angles has been driven by the following considerations: small angles require to ignore a large quantity of buffers in order to acquire the selected ones (hence requiring a long acquisition time); on the other hand small θ ensure a good similarity of the buffers that are actually used in the average process (hence ensuring a fast averaging process and improving the possibility of an early failure detection).

Table 5 shows the typical results of the time-average process with limit angle varying from 5 to 40 deg, compared with the conventional average results.

It is clearly visible that with small angles the convergence is rapidly achieved when simply looking at the number of actually used buffers, NA. On the other hand, the total number of buffers, including those discarded, becomes unacceptably large with a consequently long acquisition time.

Signal: SUN70A08				Signal: PLA70A08			
Angle (deg)	NA	TB	TC	Angle (deg)	NA	TB	TC
±5	15	642	10.6	±5	15 **(1)**	630 **(1)**	-
±7	15	375	6.2	±7	20	537	47.8
±10	20	375	6.2	±10	25	476	42.4
±13	25	366	6.1	±13	30	447	39.8
±15	30	366	6.1	±15	45	553	49.2
±17	30	308	5.1	±17	55	582	51.8
±20	30	268	4.4	±20	70	643	57.3
±25	50	357	5.9	±25	95	688	61.3
±30	65	388	6.4	±30	110	659	58.7
±40	60	264	4.4	±40	110	489	43.5
no sel.	130 **(2)**	130 **(2)**	-	no sel.	90	90	8.0

NA: number of averages to convergence
TB: total number of buffers (including those skipped)
TC: overall time to convergence (sec)
no sel. : no buffer selection (conventional averaging procedure)
(1) convergence not achieved: reached raw data EOF
(2) convergence not achieved: reached max. number of averages

Table 5: Time average results with different angles

The necessity for a very large amount of data clashes with the limited length of the available time history (700 buffers of 1024 samples) for the planet signal, preventing the achievement of the final average

with θ=±5 deg. Intermediate result of the 15th average indicates that the convergence was close to the acceptable limit, therefore it is believed that with 20 averages the convergence could be achieved. It must be however remarked, especially for θ=±5 deg, the extremely high acquisition time.

After several tests, the value of θ= ±10 deg has been finally chosen for both sun and planet, this value represent a compromise between a reasonably fast acquisition time and a good similarity of the selected buffers. In fact angles less than 7 deg, in spite of the low number of averages, require an unacceptably large acquisition time, while angles larger than 20÷25 deg do not provide a sufficient buffer similarity especially in relation to the necessity of maximizing the visibility of the defects.

The new averaging procedures yields satisfactory results, requiring an average of less than 30 cycles to achieve the convergence with both sun and planet signals. Furthermore, the convergence has been always achieved in less than 45 cycles for the sun and in less than 35 for most planet signals.

6.2 AVERAGED SIGNAL ANALYSIS

6.2.1 SIGNAL CHARACTERISTICS - SUN

As already described, the new time-average procedure allows to focus the gear health analysis on a limited sector of the sun gear. A 256 samples' buffer corresponds to about 81 deg; hence, at least 5 sectors are necessary to cover all of the 360 deg (corresponding to 1140 samples) of one gear revolution.

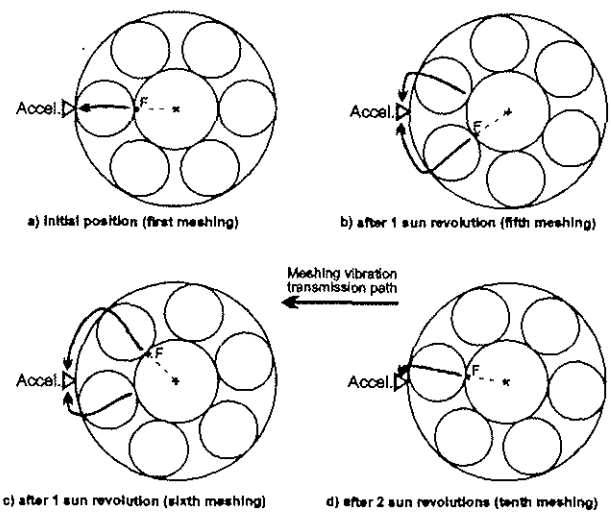

Fig.3: Sun/planet successive positions.

The analyses performed on 50% seeded fault signals highlighted that it is not sufficient to consider one sun revolution. Especially with "small" defects the meshing signal transmission path is very important: the defect is more evident when the meshing of the failed tooth occurs when it is aligned with both planet and accelerometer (see fig.3a). After a sun revolution, the meshing of the failed tooth with the planets occurs in the positions indicated in fig.3b and 3c, respectively 37 and 44 deg apart from the initial aligned position. In such a condition the signal sensed by the accelerometer is given by the sum of the failed meshing with a "normal" signal of comparable amplitude (the relative importance is related to the ratio of the angles). This effect can explain the inability to highlight the defect in such cases. After the second sun revolution, the meshing occurs close to the initial position (8 deg of angular separation, see fig.3d); the corresponding signal is predominantly given by the failed tooth and it is similar to the signal caught in the initial position. This hypothesis is confirmed by the analysis results that give comparable values with a two sun revolution periodicity.

Therefore, in order to be able to identify a "small" defect it has been chosen to analyse two sun revolutions. When using buffers of 256 samples, this choice implies to average 9 adjacent sectors. Each of them can be averaged simply by skipping N*256 samples (with N=1,2,..,8) on the raw time history and using the same sun buffer sequence as listed in appendix 1.

A further modification with respect to the original analysis procedure is imposed by the lack of periodicity of the averaged signal in each buffer, i.e., the leading and trailing extremes of the buffer do not link together, as shown in fig.4.

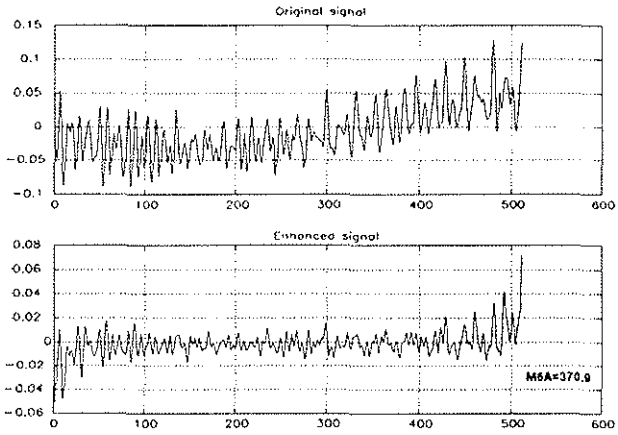

Fig.4: SUN (BAS70A08 sector 5): average with θ=±10 deg; original and enhanced signals.

The signal enhancement algorithm, which is designed to highlight any deviation from a continuous periodic signal, magnifies this discontinuity as pulses at the extremes of the buffer. The result is the computation, even with gears in good conditions, of M6A values that are closer to those associated to failed teeth, rather than the low values that are expected from normal meshing (see fig.4, where an unreliably high M6A=370.9 has been computed for a transmission in good conditions).

The application of a windowing to the enhanced signal avoid this undesired effect, lowering the M6A values computed for gears in good conditions to acceptably small values, while leaving the seeded fault results to the expected high values.

In order to make up for the loss of analysed signal at the extremes of each buffer caused by the windowing, the length of the buffer has been doubled to 512 samples (corresponding to a sun sector of 162 deg).

The size doubling provides the data overlapping which is necessary to avoid loss of data when applying the windows on the averaged signals. It also allows to slightly increase the buffer separation in the time average procedure. The choice of a buffer separation of 285 samples, corresponding to about 90 deg, instead of the former 256 (81 deg), requires 8 buffers instead of 9 to analyse two complete sun revolutions, while retaining all of the original capabilities of revealing possible defects on any tooth of the gear.

Both buffer size doubling and separation increase do not affect the selection of the acceptable buffers, which remain as listed in table 3.

Several window shapes have been tested to come to the final choice. When considering the constraint that the central portion of the buffer should not be altered, the parameters that can be modified to optimize the window refer to its sides, i.e., the two parts of the window joining its central part (value=1) with the extremes (value=0): the investigations mainly concentrated on both shape and width of the window sides.

The finally chosen shape is depicted in fig.5, together with the two adjacent windows (separated by 285 samples). The central flat portion of the window keeps the enhanced signal unchanged, while the two $\cos^2$ shaped extremes lower any pulse located close to the edge of the buffer and provide a smooth transition with the flat portion.

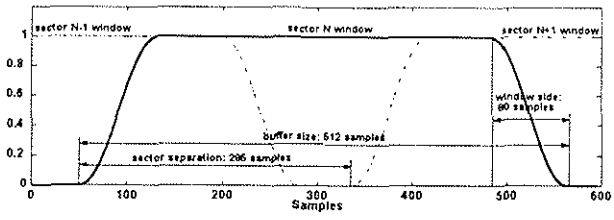

Fig.5: Sun: Window shape

In order to prevent possible data losses, due to an excessive windowing, the width of each $\cos^2$ shaped side is limited to 80 samples, allowing a sufficient overlapping of the signal with the adjacent buffers.

The possibility of deleting a pulse actually related to a tooth damage occurring at the edges of the buffer should not worry, because the same damage will be present in one of the adjacent buffers where, shifted by 285 samples and close to the centre of the buffer, it will not be modified by the window.

The capability to highlight a failure pulse is proved by the following test, where a sweep in the initial position of the raw time-history is performed. The 8 sun sectors have been averaged with an initial skip of data from 0 to 250 samples with a step of 50.

The aim of the test is to prove that, regardless of the initial position of the averaging procedure, there will always be at least one sector with a well recognizable pulse and giving a sufficiently high M6A value. The 285 samples skip case has been included for completeness. In fact, shifting 285 samples in the time history is equivalent to performing again all of the 0-shift averages except the first one (which is not performed) and the last one (which is performed instead of the first and should be nearly equivalent). When considering this aspect it should not surprise that sectors 2 through 8 of the zero-shift averages are exactly the same as sectors 1 through 7 of the 285-shift case (the M6A values reflect this property).

Among the performed test, only the one with the 50% seeded fault (accel. 8) is reported in this document. It is the most interesting case since the pulse is not so evident as the 70% seeded fault is but, unlike the 20% case, it is still recognizable.

Table 6 shows the position sweep results, analysed according to the procedures described in the following paragraph.

It is evident from the table that, regardless of the initial averaging position, there is always at least one sector with an M6A value sufficiently high as compared to the baseline values, whose range goes from 25 to 40.

Sweep (samples)	0	50	100	150	200	250	285
Sector 1	**119.6**	**148.9**	**161.6**	36.8	23.6	26.5	18.5
Sector 2	18.5	27.9	30.3	15.3	19.4	37.9	25.1
Sector 3	25.1	29.9	32.7	47.7	28.0	34.2	46.2
Sector 4	46.2	22.3	18.0	22.9	38.7	49.7	64.2
Sector 5	64.2	**122.0**	34.9	37.6	50.7	47.2	41.6
Sector 6	41.6	98.7	**189.6**	**198.7**	**166.2**	52.9	18.8
Sector 7	18.8	14.9	19.6	22.3	26.0	21.9	14.8
Sector 8	14.8	**176.8**	**112.9**	87.0	**118.3**	**140.8**	**165.2**

Table 6: SUN50A08, analysis results with initial position sweep

The highlighted defect initially falls in sector 1. When the averaging initial position is moved forward in the raw time history the defect drifts towards sector 8 (note that with 50 and 100 samples sweeps the defect is highlighted in both sectors 1 and 8). When the sweep is greater than 100 samples the defect is evident only in sector 8.

It is interesting, and not completely explainable, that high M6A values are present in sectors 5 and 6, where the meshing of the seeded fault occurs far from the accelerometer. Though a precise explanation has not yet been found, it is believed that such effect can be related to signal enhancements due to particular vibration transmission paths.

It is noteworthy that the same effect, with the same buffer sequence has been found also with 70% seeded fault recordings.

Table 6 confirms that 4 sectors are not sufficient to highlight small defects, in fact with sweeps greater than 100 samples the first 4 sectors do not give any evidence of a failed tooth; it is necessary to monitor a second sun revolution to highlight the presence of the seeded fault.

The 70% seeded fault case gives similar results apart from a different failure location, higher M6A values and the capability to highlight the defect in a larger number of sectors.

The 20% seeded faults and baseline recordings give M6A values that are low, as expected, and almost constant regardless of the average initial position.

It can be concluded that the described averaging and windowing procedure are appropriate to highlight the presence of medium to large failures (at least 50% seeded fault) regardless of the initial acquisition position.

6.2.2 SIGNAL ENHANCEMENT - SUN

The analysis algorithms used in the enhancement procedure are similar to those already available and used up to now. The effectiveness of these algorithms, when applied to signals where the averaging process is properly applied to retain all of the important characteristics of the signal, requires only a tailoring aiming at the optimization of the enhancement process.

The major modification of the algorithm is the introduction of a preventive high-pass filtering at order 10, aimed at removing the low frequency oscillations that are synchronous with the planet passage in front of the accelerometer (see fig.1). These low frequency oscillations are partly removed in the enhancement process (the corresponding lines in the spectrum were selected and consequently lowered, but a limited amplitude oscillation still remains in the enhanced signal). Its effect is mainly to increase the variance of the enhanced signal, thus lowering the M6A values especially in the averaged buffers with faults. The cancellation of the spectrum below order 10 eliminates this negative effect without deleting any important information about possible failures, which are located at medium and high frequencies.

After this high-pass filtering, the remaining enhancement process is a conventional application of the enhancement algorithm.

The value of the algorithm parameters has been chosen in order to maximize the M6A values computed with seeded fault recordings, while keeping the "baseline" values below a reasonably low threshold.

The described window with $\cos^2$ shaped edges and a flat portion of 348 samples (fig.5) is applied after the signal enhancement process.

Baseline recordings			Seeded fault recordings		
	M6A			M6A	
Ref. name	Max	Min	Ref. name	Max	Min
PP7SLA08	25.6	12.6	SUN20A08	23.0	12.4
PP7SLA09	28.5	15.5	SUN20A09	22.6	11.2
PP7SLA10	27.4	14.7	SUN20A10	28.7	13.3
PP7SHA08	27.7	11.4	SUN20A82	23.2	13.6
PP7SHA09	33.8	12.2	SUN20A83	33.2	17.1
PP7SHA10	25.4	11.7	SUN50A08	**119.6**	14.8
PP2SLA08	27.0	13.0	SUN50A09	**109.5**	18.0
PP2SLA09	21.0	14.8	SUN50A10	**112.4**	18.0
PP2SLA10	39.7	14.6	SUN50A82	**119.7**	25.3
PP2SHA08	25.5	14.2	SUN50A83	**265.1**	13.6
PP2SHA09	28.9	13.5	SUN70A08	**368.0**	23.8
PP2SHA10	17.8	14.0	SUN70A09	**168.8**	15.0
PP6SHA08	23.1	12.5	SUN70A10	**236.6**	33.3
BAS20S08	31.2	10.8	SUN70A82	**174.6**	10.9
BAS20S09	22.6	12.4	SUN70A83	**266.0**	33.7
BAS20S10	22.9	10.5			
BAS20S82	33.5	14.8			
BAS20S83	33.3	15.6			
BAS70S08	37.2	14.6			
BAS70S09	26.6	15.7			
BAS70S10	19.2	13.3			
BAS70S82	23.2	16.7			
BAS70S83	24.2	14.0			

Table 7: SUN analysis results; maximum and minimum M6A values.

The final analysis results are shown in table 7, which lists both the maximum and minimum of the eight M6A values for each signal (only the maximum M6A value is considered for health analysis purposes).

It is clear how the improved procedure can highlight both 70% and 50% seeded faults; the values of M6A computed in these cases are well separated from the baseline ones (the highest M6A value for the baseline recordings is 39.7, while the lowest M6A value for the 50% seeded fault is 119.6, i.e., almost 3 times greater). This large difference gives some confidence in the selection of the maintenance and warning thresholds.

Unfortunately, the 20% seeded fault values are not discernible from the baseline values. At this stage of the research, the developed algorithms can not discriminate between a gear in good conditions and one with a very small fault. However, it should be noted that the removal of the 20% of the tooth casehardening surface does not significantly affect the meshing vibration signal; the M6A values never indicated a possible presence of the defect.

6.2.3 SIGNAL CHARACTERISTICS - PLANET

The buffer selection performed by the new time average algorithm allow to focus the planet analysis on a single planet gear when its meshing occurs close to the accelerometer. To this purpose, the buffers listed in table 4 must be averaged together to come to first planet average. The signal averages of planets 2 through 6 are obtained by shifting each time 548 samples in the raw time history for each planet and averaging with the same sequence.

Considering the size of the planet buffer (1024 samples) it is evident a 476 samples overlapping with each of the adjacent buffers.

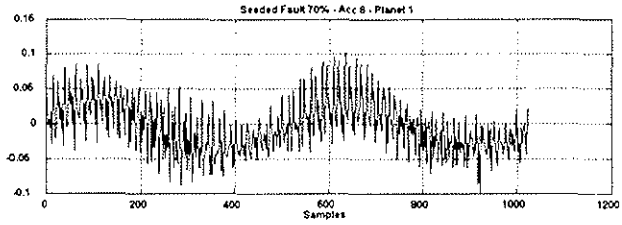

Fig.6: Planet averaged signal

Fig. 6 presents a typical result of a planet average. Some of the already described sun signal characteristics are also present in the planet averages.

The low frequency oscillations that are related to the planet passage in front of the accelerometer require also in this case the application of a high pass filter at order 10.

Again, the windowing of the averaged signal is necessary to remove the discontinuities at the extremes of the buffer and to compensate its lack of periodicity.

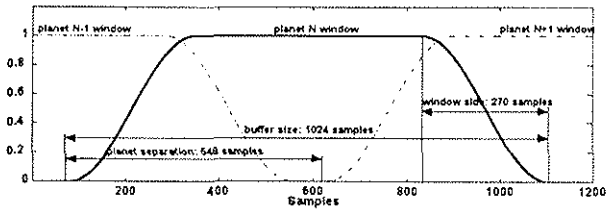

Fig.7: Planet: Window shape

The performed analyses indicated that it is desirable to maximize the width of the window sides.

The chosen window is shown in fig.7: the window sides are $\cos^2$ shaped and each one is 270 samples width. The selected side width is slightly larger than the maximum value of 238 samples that guarantees no attenuation in any part of the signal but, because of the slow roll-off of the window, the signal attenuation between adjacent buffers is very limited (see fig.7).

The definitive proof of the capability to detect a possible failure regardless of the initial sampling point (and therefore of the absence of data losses) is given by the results of the analyses with a shift on the initial position. As described for the sun, the same raw time history has been averaged with slightly different initial positions (from 0 to 500 with 50 samples' steps).

As for the sun, the 50% seeded fault (accel. 8) analysis results are reported in table 8. It is evident how at least one of the six planets is characterized by high M6A values. As expected, the forward shift of the initial averaging position causes the shift of the defect pulse from the initial planet 6 to the planet 5.

Note that a 548 samples' shift corresponds, with respect to the zero samples shift, to a complete transposition of the averaged signal (and therefore of the M6A) from a planet to the preceding one, with the exception of the sixth that is merely similar to the first one.

Shift (samples)	0	50	100	150	200	250
Planet 1	20.3	23.8	25.8	25.4	28.1	28.3
Planet 2	29.5	40.4	41.7	41.1	43.5	51.7
Planet 3	20.4	21.5	25.2	21.3	20.6	24.0
Planet 4	30.1	29.8	28.6	28.4	34.1	36.1
Planet 5	25.4	32.3	33.7	53.2	**151.9**	**193.1**
Planet 6	**198.5**	**229.4**	**234.7**	**229.4**	**268.3**	**144.2**
Shift (samples)	**300**	**350**	**400**	**450**	**500**	**548**
Planet 1	20.0	30.7	39.4	28.2	26.7	29.5
Planet 2	45.8	48.6	37.3	18.8	18.9	20.4
Planet 3	23.7	26.5	27.7	30.4	29.9	30.1
Planet 4	25.4	17.9	15.1	27.8	34.2	25.4
Planet 5	**186.9**	**189.3**	**222.3**	**242.4**	**209.6**	**198.5**
Planet 6	30.6	24.8	24.3	21.0	23.2	24.1

Table 8: PLA50A08, analysis results with initial position sweep

Similar results are obtained with 70% seeded faults (in this case the defect is visible in more than one planet average), while baseline analyses give almost constant low M6A values when varying the initial position.

6.2.4 SIGNAL ENHANCEMENT - PLANET

The major modifications of the enhancement procedure are the application of both high pass filtering and signal windowing before the spectral reduction.

Several combinations of both number of lowered harmonics and low pass filter cutoff order have been tested (together with the window characteristics) in order to maximize the separation between the analysis results of the baseline recordings and those of the seeded faults.

Apart from the window width, the finally chosen spectral reduction parameters are closely related to those already selected for the sun analyses.

Table 9 presents both maximum and minimum M6A values for each signal (only the maximum M6A value is considered for health analysis purposes). The listed results are satisfactory: the baseline signals give maximum M6A values that are generally below 45, while 50 and 70% seeded values are at least 3 times larger.

Baseline recordings			Seeded fault recordings		
	M6A			M6A	
Ref. name	Max	Min	Ref. name	Max	Min
PP7PLA08	25.8	17.2	PLA20A08	23.3	16.9
PP7PLA09	35.8	19.1	PLA20A09	26.8	19.2
PP7PLA10	63.3	20.6	PLA20A10	29.9	17.1
PP7PLA1B	37.5	20.0	PLA20A82	41.5	20.6
PP7PHA08	27.4	18.5	PLA20A83	25.7	20.8
PP7PHA09	29.8	21.5	PLA50A08	**198.5**	20.3
PP7PHA10	23.4	16.6	PLA50A09	85.1	17.1
PP2PLA08	33.2	15.3	PLA50A10	**154.2**	16.1
PP2PLA09	33.2	20.6	PLA50A82	**162.6**	18.6
PP2PLA10	42.1	19.7	PLA50A83	31.7	16.4
BAS20P08	25.1	18.1	PLA70A08	**294.4**	19.6
BAS20P09	30.4	19.5	PLA70A09	**224.5**	17.0
BAS20P10	25.6	14.9	PLA70A10	**132.2**	16.2
BAS20P82	26.7	16.1	PLA70A82	**325.8**	21.6
BAS20P83	31.8	17.5	PLA70A83	**3058.7**	24.1
BAS70P08	26.2	17.7			
BAS70P09	28.8	20.2			
BAS70P10	23.8	17.4			
BAS70P82	25.4	18.5			
BAS70P83	43.2	18.3			

Table 9: PLANET analysis results; maximum and minimum M6A values.

There are three exceptions to this trend:

PP7PLA10: planet 5 gives an M6A value of 63.3. Though not comparable with 50 and 70% seeded fault results, this value is higher than the usual baseline results. Comparably high M6A values have been found with almost any combination of analysis parameters, but it is believed that this is an anomalous result, not related to an actual failure. The second analysis performed on the same signal (PP7PLA1B) gives normal M6A values. It should be noted that the false alarm management implemented on the TVM device prevents the rising of an alarm if the computed M6A do not exceed in two consecutive analyses the prescribed limit threshold.

PLA50A09: the computed M6A value is rather low (85.1), especially when compared to other accelerometer results. Accelerometer 9 signals are characterized by lower M6A values in the seeded fault analyses. This negative behaviour should not worry since 8 and 10 have been respectively selected as primary and secondary accelerometers in the epicycle gear analyses.

PLA50A83: this analysis result is surprisingly low: the maximum M6A value is 31.7, well below the other 50% seeded fault values.
Unfortunately it is not possible to repeat the raw time history acquisition since the original tape is damaged and the recorded data are not trustworthy. It is even possible that also the data used for the described analysis are not completely reliable.

As for the sun, 20% seeded fault results are not separated from other baseline values; the current algorithms do not allow the recognition of such little defects.

The listed values provide preliminary information on the expected range of the analyses' results. The noticeable separation between baseline and seeded fault results gives some confidence for the alarm thresholds' selection, that however shall be confirmed by further analyses, especially on data coming from helicopters and Ground Test Vehicle.

8. CONCLUSION

The epicyclical gears analysis presents some peculiar characteristics, when compared to the conventional two gear stage health monitoring: the complexity of its vibrational signal requires dedicated procedure to achieve the desired effectiveness in the early failure detection capability.

An analysis method has been developed, tested and presented here together with the first results, which are believed encouraging.

Some refinements or simplifications of the algorithms can be expected in the final implementation, both as a consequence of further evaluation and in order to optimize the hardware requirements of the procedure.

The future efforts shall be mainly dedicated both to the enlargement of the data base (especially with signals recorded on the prototypes and on the Ground Test Vehicle) and to the continuous refinement of the developed algorithms, with a possible inclusion of improved filtering techniques and alternative solutions for the signal windowing and analysis.

REFERENCES

1. P.D. McFadden and J.D. Smith, An explanation for the asymmetry of the modulation sidebands about the tooth meshing frequency in epicyclic gear vibration, Proc. Inst. Mech. Eng. Vol. 199 N° C1.

2. D.R. Houser and M.J. Drosjack, Vibration signal analysis techniques, USAAMRLD Technical Report 73-101.

3. P.D. McFadden, Examination of a technique for the early detection of failure in gears by signal processing of the time domain average of the meshing vibration, Mechanical systems and signal processing Vol 1 No 2, 1987.

4. P.D. McFadden, A revised model for the extraction of periodic waveforms by time domain averaging, Mechanical systems and signal processing Vol 1 No 1, 1987.

5. D.A. Dousis, A vibration monitoring acquisistion and diagnostic system for helicopter drive train bench tests. AHS 48th annual forum proceedings, June 1992.

6. P.D. McFadden, detection of fatigue cracks in gears by amplitude and phase demodulation of meshing vibration, Journal of vibration, acoustics, stress, and reliability in design, Vol. 108, April 1986.

7. J.T. Broch, Mechanical vibration and shock measurements, Bruel and Kjær, 1984.